Solar Energy Materials & Solar Cells 131 (2014) 46–50

Contents lists available at ScienceDirect

Solar Energy Materials & Solar Cells

journal homepage: www.elsevier.com/locate/solmat

Tunnel oxide passivated contacts as an alternative to partial rear contacts

Frank Feldmann*, Martin Bivour, Christian Reichel, Heiko Steinkemper, Martin Hermle, Stefan W Glunz

Fraunhofer Institute for Solar Energy Systems ISE, Heidenhofstrasse 2, 79110 Freiburg, Germany

ARTICLE INFO

Article history:
Received 15 April 2014
Received in revised form
20 May 2014
Accepted 5 June 2014
Available online 10 July 2014

Keywords:
Passivated contact
Passivation
PERC
PERL
High-efficiency

ABSTRACT

Recently, n-type Si solar cells featuring a passivated rear contact, called *TOPCon* (Tunnel Oxide Passivated Contact) were reported. The high conversion efficiency of 24.4% and very high *FF* > 82% demonstrates that the efficiency potential of this full-area passivated rear contact is as good as or even better than that of partial rear contact (PRC) schemes like PERL (passivated emitter and rear locally diffused) and in addition avoids complex structuring steps and features a 1D carrier transport. Likewise, a boron-doped passivated rear contact for p-type solar cells (p-TOPCon) is proposed as an alternative to p-PRC cells. The optimum device design of PRC cells has to account for two opposing effects: a low-loss 3D carrier transport requires a high base doping but Shockley–Read–Hall (SRH) recombination within the base due to the formation of boron–oxygen complexes in standard Cz silicon calls for a low base doping level. This conflict might be overcome by p-TOPCon because its performance is less sensitive to base doping. This will be discussed on the base of experimental results. It is shown that its high implied fill factor (*iFF*) of 84% combined with the 1D carrier transport in the base translates into a higher *FF* potential. First investigations on planar solar cells prove the good performance of the p-TOPCon with respect to passivation and carrier transport. A V_{oc} of 694 mV and a *FF* of 81% underline the efficiency potential of this rear contact.

1. Introduction

Today the industry is working towards the implementation of PRC [1] schemes in production. Recombination at the local metal-semiconductor contacts is a major source of device recombination which is significantly reduced by simply decreasing the metallized area fraction. However, V_{oc} and *FF* losses – the latter arise in particular from the 3D carrier transport at the rear (Fig. 1, left) – have to be carefully balanced by adjusting the pitch of the point contacts. For industrial p-type Cz silicon device optimization is even more complex because a low series resistance R_S, which requires high base doping for an efficient 3D transport, comes at the expense of significant SRH recombination caused by light-induced degradation (LID) [2]. Thus, the formation of boron–oxygen complexes constitutes a major efficiency limitation for these devices.

An appealing alternative to a point contact structure is a full-area passivated contact which decouples the absorber's passivation from the local metallization. In 1985 Lindholm et al. showed for the first time that heavily-doped polysilicon contacts can reduce the recombination at the rear side to some extent [3]. The benefit of applying polysilicon contacts to Si solar cells in terms of V_{oc}, i.e. J_{0e} was also demonstrated by others [4–6] and was recently revisited by Borden et al. (p^+-polysilicon/c-Si(n) junction) [7]. In contrast to a-Si:H based heterojunctions the polysilicon contacts are a viable option for conventional solar cells due to their higher tolerance to high-temperature processes. For instance, in Ref. [3] the polysilicon contacts were first realized on the rear side, then capped by a protective layer, and finally exposed to a diffusion process forming the front emitter.

In this work so-called tunnel oxide passivated contacts (TOPCon) for n-type as well as p-type Si solar cells are discussed. The TOPCon structure resembles the polysilicon contacts with deliberately grown interfacial oxide. In contrast to the polysilicon contacts, the TOPCon structure employs a wide bandgap semiconductor layer which contains amorphous and crystalline Si phases. For more details on the contact's morphology and structure as well as its implications on the blue response (parasitic absorption) the reader is kindly referred to Ref. [8].

The paper first addresses the passivated electron contact which was recently disclosed [9]. Due to its excellent carrier selectivity it enables high V_{oc} and *FF* at the same time which was demonstrated on an n-type Si solar cell featuring a boron-diffused emitter and

* Corresponding author. Tel.: +49 7 61 45 885287; fax: +49 7 61 45 889000.
E-mail address: frank.feldmann@ise.fraunhofer.de (F. Feldmann).

http://dx.doi.org/10.1016/j.solmat.2014.06.015
0927-0248/

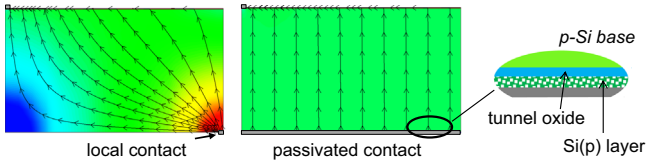

Fig. 1. Simulated current density of solar cells with local rear contacts and a passivated rear contact, respectively. The arrows indicate the minority carrier flow pattern.

the phosphorus (P)-doped passivated rear contact. In addition, its simple device design enables a 1D current flow in the base and thereby avoids *FF* losses originating from a 3D carrier transport (Fig. 1, right). Furthermore, it showed a high thermal stability and therefore could be integrated into a conventional diffused solar cell. Likewise, a boron (B)-doped passivated contact for p-type Si solar cells is proposed as an alternative to p-PRC cells which is investigated in more detail. Due to its one-dimensional device design, it might enable the use of lowly-doped wafers. Therefore, p-type cells featuring this passivated rear contact might be less prone to light-induced degradation. To this end, the interface passivation of p-TOPCon is studied on highly and lowly-doped p-type Si. Especially the implied *FF* (*iFF*), which describes the injection-level dependence of the passivation, will be discussed and compared to rear side passivation layers typically applied to p-PRC cells. Thereafter, the dark band bending, φ_0, induced by the passivated contact in the c-Si base is probed by means of the surface photovoltage (SPV) technique. It is a measure for the generated built-in potential V_{bi} of the p-TOPCon/c-Si(n) junction and can be used as an indicator for sufficient doping of the hole contact. Third, the passivated rear contact is integrated into a solar cell featuring n-TOPCon as emitter to facilitate the demonstration of its high V_{oc} and *FF* potential.

2. The passivated rear contact for n-type Si solar cells

The n-TOPCon rear contact for n-type Si solar cells [9] features a tunnel oxide grown in a nitric acid bath [10] and a P-doped Si layer. After deposition of the amorphous Si layer the contact is annealed at temperatures in the range of 800 °C to 900 °C and subsequently exposed to a 30-min hydrogen passivation process at 400 °C (remote plasma hydrogen passivation (RPHP)) [11]. Fig. 2 depicts the injection-dependent carrier lifetime curve for the n-contact after annealing at 800 °C and subsequent hydrogen passivation for symmetrical Si(n)/SiO_x/c-Si(n)/SiO_x/Si(n) samples. A high implied V_{oc} of 725 mV was obtained and corresponds to $J_{0,rear} \approx 7$ fA/cm². The J_0 values were calculated in the same manner as did in Ref. [9], where also the shortcomings of this method were discussed. However, this method is still very useful to later weigh the impact of front and rear recombination on the cell's V_{oc}. To assess the recombination limited *FF* potential of the passivated contact the *iFF*, which is a direct measure of the minority carrier recombination at maximum power point (MPP) conditions [12] is the relevant parameter for the electrical quality of the contact. The *iFF* is obtained in a similar manner as the pseudo *FF* (*pFF*) from SunsV_{oc} measurements [13] by using an implied *J*–*V* curve with the distinction that the iV_{oc} – calculated from the $\tau_{eff}(\Delta n)$ curve – is used instead of the V_{oc}. The difference between measured effective lifetime and the intrinsic limit, defined by the Auger recombination, is a measure of the quality of the passivated contact. Since the Auger limit is considerably higher at MPP than at open-circuit (OC) conditions, it is more difficult to approach this limit, i.e. obtain a very low minority carrier recombination at MPP, too. In this case a very high *iFF* larger 86% was obtained and underlines the excellent

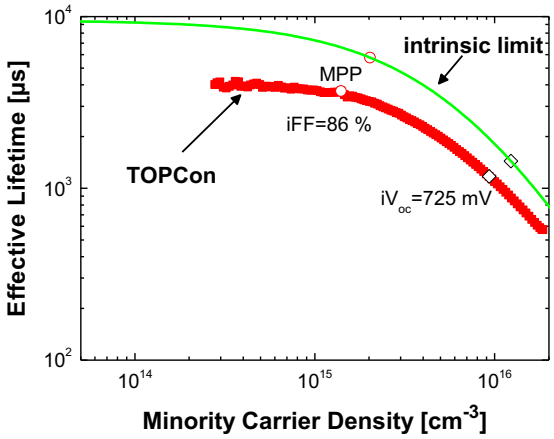

Fig. 2. Injection-dependent carrier lifetime curve of n-TOPCon after annealing at 800 °C, 1 h and hydrogen passivation.

Table 1
Overview of the champion efficiency of each solar cell generation. The n-type solar cells feature a boron-diffused emitter and the tunnel oxide passivated rear contact. The solar cell results except for the *pFF* were independently confirmed by Fraunhofer ISE Callab. The cell area is 2 × 2 cm² and the measurement condition is aperture area.

	V_{oc} (mV)	J_{sc} (mA/cm^2)	*FF* (%)	*pFF* (%)	η (%)
Gen 1	690.8	38.4	82.1	84.3	21.8
Gen 2	698.1	40.6	81.1	84.0	23.0
Gen 3	703.2	41.4	82.5	84.7	24.0
Gen 4	**715.1**	**41.5**	**82.1**	**85.0**	**24.4**

interface passivation over a wide injection range and thus a high *FF* potential of n-TOPCon.

The n-contact then replaced the locally diffused point contact passivation scheme of a high-efficiency n-type Si solar cell with boron-diffused emitter (140 Ω/sq) [14]. The development of these TOPCon cells is outlined and the light *I*–*V* and SunsV_{oc} [13] parameters of each generation's champion cell are given in Table 1.

Due to TOPCon's low contact resistance of ~10 mΩ/cm² and the cell's high *pFF* > 84%, high *FF*s above 82% were already obtained with the first generation. Thus, the *FF* gain compared to a similarly fabricated PERL cell is ~1% absolute [14]. Yet a strong parasitic absorption of light at the rear metal contact (titanium) caused a significantly lower J_{sc} [9] and, therefore, the maximum efficiency was just 21.8% (see Table 1). The insufficient light trapping
scheme was improved in a second generation (Gen 2) by replacing titanium with a silver rear contact resulting in a champion efficiency of 23.0%. A slightly higher V_{oc} was obtained by a reduction of the contact area of the metal front contacts from ~3% down to ~1.1%. However, the very high FF was partially sacrificed due to the poor contact resistance at the metal-emitter contact (ρ_c ~ 9 mΩ/cm²). This series resistance contribution was drastically diminished in a third generation (Gen 3) by replacing the Ti/Pd/Ag metal stack for a Pd/Ag stack at the front. Owing to a low contact resistance below 1 mΩ/cm², the contact area could be reduced to ~1.1% enabling a high V_{oc} > 700 mV without sacrificing the high *FF* obtained in Gen 1. Therefore, excellent *FF*s of up to 82.5% were attained. In combination with some minor processing improvements, a champion cell with 24.0% conversion efficiency was achieved.

Although the n-TOPCon rear side provided excellent passivation quality, the V_{oc} of the Gen 3 cells is still similar to that of a PERL cell [14]. This can be ascribed to the recombination at the

unpassivated metal-semiconductor front contacts which pose the major drawback of this cell concept in terms of V_{oc}. To illustrate this point, a V_{oc} loss analysis using the simple one-diode model is carried out according to Eq. (1):

$$V_{OC} = \frac{kT}{q} \ln\left(\frac{J_{sc}}{J0e + J0b} + 1\right) \quad (1)$$

The contribution from the base and n-TOPCon rear contact amounted to about $J_{0b} \approx 20$ fA/cm² ($J_{0,rear} \approx 7$ fA/cm², $J_{0,Auger,c\text{-}Si} \approx 13$ fA/cm²). While the p^+-emitter was well passivated by Al_2O_3 and took a low value of $J_{0,pass} \approx 11$–15 fA/cm², the unpassivated metal-semiconductor contacts contributed significantly to device recombination. Using the simulation program EDNA [15] $J_{0,metal} \approx 1600$ fA/cm² ($S_{metal} = 10^7$ cm/s, $T = 300$ K) was obtained and for ~1.1% metallized area the total J_{0e} took a value of about 30 fA/cm². As a result the V_{oc} of the solar cell was limited to about 705 mV which is in agreement with the experimental results. In order to reduce this V_{oc} loss, a selective emitter underneath the metal contacts was introduced to screen the minority carriers in the emitter. Needless to say, Auger recombination in this heavily-doped p^{++}-area ($R_{sheet} = 10\ \Omega$/sq, $N_{surf} = 2.7 \times 10^{19}$ cm^{-3}) was considerably increased. On the other hand, the recombination at the metal-semiconductor contact, $J_{0,metal}$, was significantly reduced from 1600 to about 200 fA/cm² (determined from unpassivated p^{++}/c-Si(n)/p^{++} samples). Therefore, the total emitter saturation current density took a low value of about 13–17 fA/cm² which yielded $V_{oc} \approx 714$ mV. As can be seen from Table 1, the simulated finding matches the experimental solar cell results (Gen 4) well. Hence, with the selective emitter a record conversion efficiency of 24.4% was achieved. Still minority carrier recombination is higher at the front side than at the rear side. In order to fully benefit from the potential of the n-TOPCon, passivated metal-semiconductor front contacts have to be implemented and the emitter passivation has to be improved even further. However, a further reduction of J_{0e} is only expected for emitters with an even lower surface concentration.

3. The passivated rear contact for p-type Si solar cells

After we have demonstrated the excellent efficiency potential of n-TOPCon, in the following we will focus on its boron-doped counterpart, p-TOPCon, for p-type Si solar cells. From a scientific point of view a comparison of both contacts might be interesting and reveal some technological differences. For instance, significantly lower J_{0e} values were reported for in-situ doped n^+-polysilicon/c-Si junctions (20 fA/cm² [16]) than for p^+-polysilicon/c-Si junctions (~100 fA/cm² calculated from the Gummel number[1] G_E given in [17] and $n_i = 1.1 \times 10^{10}$ cm^{-3}). Therefore, the reported current gain enhancement was typically larger in the case of npn transistors than pnp transistors. Several explanations for this distinctive behavior were given but as of today there is no evidence for a fundamental difference between these two types of junctions. And indeed, Gan and Swanson showed that very low J_{0e} can be obtained for both n^+-polysilicon/c-Si and p^+-polysilicon/c-Si junctions [5]. This approach, which involves at least two high-temperature anneals, was recently revisited by Roemer et al. [18].

One aspect which makes the fabrication of p-TOPCon more challenging might be defect creation of defects in the tunnel oxide layer by diffusing boron atoms during the high-temperature anneal [19]. Furthermore, B-doped amorphous silicon films presumably exhibit a higher defect density than P-doped amorphous silicon films which in essence can be a problem for a-Si:H based heterojunctions [20].

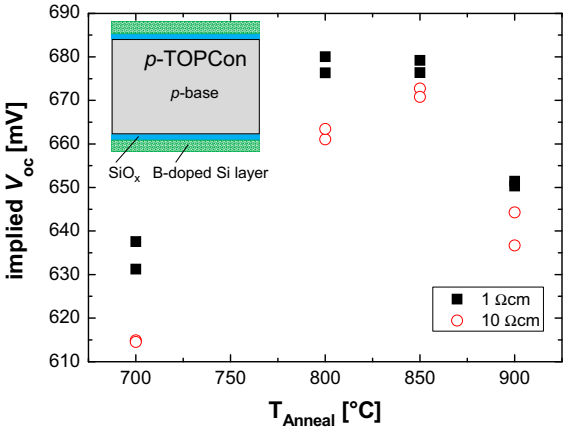

Fig. 3. The implied V_{oc} as a function of the thermal activation anneal.

Within the next sections first results regarding p-TOPCon's interface passivation on highly- and lowly-doped c-Si are presented. The band bending induced into c-Si by the contact is studied for moderately and strongly-doped Si layers and finally, the contact's carrier selectivity is investigated on a simple solar cell test structure.

3.1. Interface passivation quality

The passivation quality of p-TOPCon was tested for by lifetime measurements. 250 μm thick (1 0 0)-oriented shiny-etched p-type FZ wafers with base resistivities of 1 and 10 Ω cm were used, respectively. After an RCA clean a ~14 Å thin tunnel oxide layer was wet-chemically grown in 68 wt% nitric acid and capped by a 15 nm thick boron-doped amorphous Si layer on both sides. Subsequently, the samples underwent a furnace anneal with plateau temperatures of $T_{Anneal} = 700$–900 °C. Following the furnace anneal, the samples were subjected to a 30-min hydrogen passivation process in an atomic hydrogen atmosphere at 400 °C (RPHP).

In Fig. 3 the iV_{oc} is plotted over T_{Anneal} for the two base resistivities. First, it can be seen that in this experiment a maximum iV_{oc} of 680 mV ($J_{0,rear} \approx 60$ fA/cm²) was obtained for the optimum temperature which is in the range of 800 to 850 °C. Second, the iV_{oc} dropped at a higher annealing temperature $T_{Anneal} = 900$ °C. At this temperature a shallow diffusion ($N_{surf} \approx 1 \times 10^{19}$ cm^{-3}, $d = 200$ nm) of boron atoms into the base was observed. However, Auger recombination ($J_{0,Auger} \approx 2$ fA/cm² determined by EDNA) and bandgap narrowing in this strongly doped Si region did not significantly contribute to minority carrier recombination and, therefore, one can conclude that the oxide's integrity might be weakened during the anneal at 900 °C. Third, the contact's passivation quality showed a slight dependence on base doping: the iV_{oc} obtained for 10 Ω cm p-type Si were lower for each annealing temperature and the optimal temperature range seems to be narrower. Still the anneal at 850 °C yielded a maximum iV_{oc} of 670 mV ($J_{0,rear} \approx 90$ fA/cm²) which is competitive with state-of-the-art PERC cells ($J_{0,rear} = 86$ fA/cm²) [21].

As for n-TOPCon, p-TOPCon must also provide low interface recombination at MPP conditions to enable high *FF*s. Fig. 4 plots the corresponding *iFF* over T_{Anneal} after the hydrogen passivation process. For the optimum annealing temperature a high *iFF* of 84.5% and 84.3% on 1 and 10 Ω cm base material was obtained, respectively. That the passivation provided by p-TOPCon depended only moderately on the base doping level and was hardly affected

[1] The emitter Gummel number is inversely proportional to the transistor's base current and is a useful figure of merit for the emitter's injection efficiency. The relation between emitter Gummel number G_E and J_{0e} is $J_{0e} = qn_i^2/G_E$.

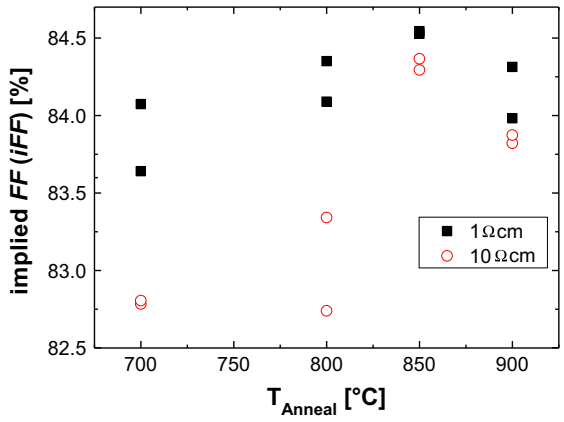

Fig. 4. The corresponding implied *FF* for the different annealing temperatures.

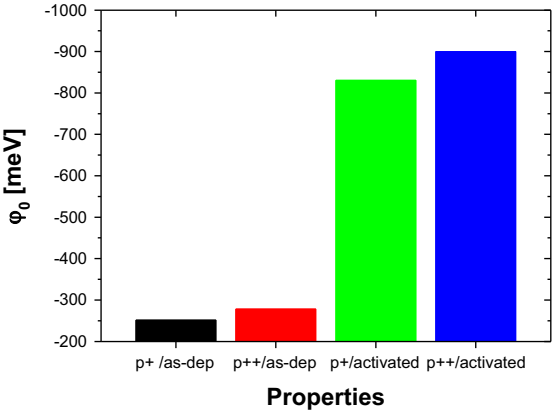

Fig. 5. Dark band bending of Si(p)/SiO_x/c-Si(n) emitter structure determined by SPV method plotted for different doping levels after deposition and after annealing at 900 °C and hydrogen passivation (denoted as activated).

by the injection-level is a very important finding. For instance, Aberle et al. showed that the recombination at the SiO_2 rear passivation layer of PERL cells was strongly increased at MPP conditions. This *FF* limitation could be ascribed to the large asymmetry in capture cross-sections ($\sigma_n \gg \sigma_p$) of the SiO_2 passivation and was more pronounced the lower the base doping [22]. Also SiN_x is not a viable option because its large number of positive fixed charges causes inversion-layer shunting at the rear side adversely affecting the *FF* as well [23]. On the other hand, Al_2O_3 based passivation schemes do not suffer from increased recombination at MPP conditions due to an accumulated surface provided by the high density of negative fixed charges [24,25]. Still PRC cells featuring an Al_2O_3 passivation scheme cannot utilize lowly-doped base material due to geometrical constrains which do not arise for a full-area passivated contact. Although the first generation of the full-area passivated p-TOPCon contact did not yield a significantly reduced minority carrier recombination compared to Al_2O_3-based PRC schemes, it might prove superior in terms of *FF* due to its one-dimensional structure.

3.2. Band bending in c-Si induced by the passivated contact

Besides a good interface passivation to achieve a large quasi-Fermi level splitting within the c-Si absorber, the passivated contact has to ensure a negligible gradient in the majority carrier quasi-Fermi level to obtain a high V_{oc} at the external metal contacts. For the formation of a hole-selective contact, the work function of the Si layer should approach the valence band of c-Si in order to induce a strong band bending. This can be achieved by means of high net doping, which avoids high-injection conditions in the Si layer as it can be observed for lowly-doped a-Si:H layers in Si heterojunction cells [26]. This high injection effect would lead to a significant gradient in the majority carrier quasi-Fermi level (due to recombination) and thereby reduce the external voltage at MPP and OC conditions.

The SPV technique [27] is a simple method to probe the band bending φ_0 induced by the passivated contact into c-Si. Here it is used as an indicator for the net doping of the Si(p) layer (for a-Si:H (p) see [26]). To this end, medium (p^+) and highly-doped (p^{++}) p-TOPCon structures were realized on n-type FZ Si with a base resistivity of 1 Ω cm. In order to validate this method Suns V_{oc} samples featuring n-TOPCon on the front side and p-TOPCon on the rear side were fabricated as well. The dark band bending due to the p-TOPCon structure was studied after deposition of the B-doped amorphous Si layer as well as after the high-temperature anneal and the hydrogen passivation process (denoted as activated). As can be readily seen from Fig. 5 the dark band bending induced by p-TOPCon in the as-deposited state was very low and increased only slightly with doping. Therefore, a reasonably high V_{oc} could not be measured. On the other hand, the activated passivated contacts yielded $\varphi_0 = -830$ meV in the case of a moderately doped Si(p) layer and $\varphi_0 = -900$ meV for the highly-doped Si(p) layer. The latter approached the upper limit $\varphi_{0,max}$ which is given by the distance between the Fermi level $E_{F,c\text{-}Si}$ and the valence band $E_{V,c\text{-}Si}$ and amounts to -902 meV for 1 Ω cm c-Si (n). The respective average V_{oc} obtained from the corresponding SunsV_{oc} samples was 658 mV (p^+) and 672 mV (p^{++}), respectively and correlates with the high band bending. In this case the V_{oc} was solely limited by the interface passivation provided by p-TOPCon. The steep increase of band bending after the high-temperature anneal can be ascribed to the partial crystallization of the Si(p) layer and the efficient activation of dopants. Hence, the highly-doped p-TOPCon induced a high built-in voltage V_{bi} and supported the high quasi-Fermi level splitting in the base so that the external V_{oc} almost matched the implied V_{oc}.

3.3. Majority carrier transport

Carrier transport across the polysilicon/c-Si junction featuring an interfacial oxide layer was extensively studied in the past. While some researchers favored the "oxide tunneling model" [28,29] assuming direct tunneling to be the dominant transport path, transport could also be realized via small pinholes in the oxide [5,30]. The latter theory seems plausible in the case of intentionally broken-up oxides (at $T_{Anneal} > 1000$ °C), where epitaxial regrowth of the polysilicon was observed. On the other hand, for moderate annealing temperatures up to 900 °C, no oxide break-up has been reported yet and the authors also observed a continuous oxide layer after annealing at 800 °C by TEM (not shown here). Therefore, there is good chance that tunneling might be important here. Considering the findings for thermally grown SiO_2, tunneling should be less likely for holes than for electrons due to the oxide's larger valence band offset to Si ($\Delta E_V = 4.5$ eV, $\Delta E_C = 3.1$ eV) [31]. However, for the related pnp polysilicon BJTs, significantly smaller barrier heights (0.3 eV for holes and 1.0 eV for electrons) were obtained [32]. In summary, as of today there does not exist a widely-accepted theory which explains the selectivity (transport of majority carriers and blocking of minority carriers) of polysilicon emitters. Nevertheless, the oxide integrated into p-TOPCon does not exceed the critical oxide thickness for tunneling of about 15 Å reported for the related metal-insulator-semiconductor (MIS) solar cells [33]. Thus, in principle tunneling could be an efficient transport path.

To investigate if p-TOPCon allows for an efficient majority carrier transport across the tunnel oxide layer, planar solar cells featuring the passivated rear contact and n-TOPCon as a carrier selective emitter were fabricated on 250 μm thick p-type 1 Ω cm FZ silicon wafers [34]. A maximum V_{oc} of 694 mV demonstrates that for p-TOPCon the high passivation quality could be transferred to device level. The reason for the increased V_{oc} of these solar cells compared to the lifetime samples can be ascribed to the very low recombination at the front side enabled by n-TOPCon. More importantly, a *FF* of 81.1% clearly states that the tunnel oxide did not constrict the majority carrier flow. The cells' series resistance was determined from the difference between *pFF* (83.6%) and *FF* [35] and took values as low as 0.5 Ω/cm². The high *FF* is a result of the 1D carrier transport in the base and the low recombination at MPP enabled by the passivated rear contact as well as the low contact resistances of n- and p-TOPCon. The efficiency of this first batch was limited mainly by the poor light trapping and shading at the non-textured front but clearly is an indication for the good performance of p-TOPCon as a rear contact for p-type Si solar cells.

4. Conclusion and outlook

Tunnel oxide passivated contacts for both n- and p-type Si were presented as an alternative rear contact to PRC schemes. On n-type Si the n-contact impressively demonstrates its potential and the 24.4% efficient champion cell underlines its superiority to PERL cells. First promising investigations on the boron-doped passivated rear contact for p-type Si solar cells were also presented. Its effective interface passivation was demonstrated for high and low base doping levels. Very importantly, $iFF > 84\%$ was also achieved on lowly-doped p-type Si which in combination with the 1D carrier transport presumably facilitates the utilization of high resistivity c-Si, which is less prone to LID. First investigations on cell levels demonstrated that p-TOPCon – with n-TOPCon as front emitter – enables high V_{oc}s (694 mV) and *FF*s (81%) and therefore, forms an efficient hole-selective rear contact with the p-type base. Considering also its one-dimensional junction design and high thermal stability, it might be the ideal candidate to replace PRC schemes. Nevertheless, further work is required to improve the interface passivation of p-TOPCon.

References

[1] A. Cuevas, Geometrical analysis of solar cells with partial rear contacts,, IEEE J. Photovoltaics 2 (2012) 485–493.
[2] A. Wolf, et al., Comprehensive analytical model for locally contacted rear surface passivated solar cells,, J. Appl. Phys. 108 (2010) 1–13.
[3] F.A. Lindholm, et al., Heavily doped polysilicon-contact solar-cells,, IEEE Electron Device Lett. 6 (1985) 363–365.
[4] N.G. Tarr, A polysilicon emitter solar cell,, IEEE Electron Device Lett. 6 (1985) 655–658.
[5] J.Y. Gan, R.M. Swanson, Polysilicon emitters for silicon concentrator solar-cells,, in: Conference Record of the Twenty First IEEE Photovoltaic Specialists Conference—1990 vols 1 and 2 (1990) 245–250.
[6] Y. Kwark, et al., Low J. contact structures using sipos and polysilicon films,, Proceedings of the 18th IEEE Photovoltaic Specialists Conference (1985) 787–792 (Las Vegas, Nevada, USA).
[7] P. Borden, et al., Polysilicon tunnel junctions as alternates to diffused junctions,, Proceedings of the 23rd European Photovoltaic Solar Energy Conference, Valencia, Spain (2008) 1149–1152.
[8] F. Feldmann, et al., Efficient carrier-selective p- and n-contacts for Si solar cells,, Sol. Energy Mater. Sol. Cells, vol. to be published (2014).
[9] F. Feldmann, et al., Passivated rear contacts for high-efficiency n-type Si solar cells providing high interface passivation quality and excellent transport characteristics,, Sol. Energy Mater. Sol. Cells 120 (2014) 270–274 (Part A).
[10] H. Kobayashi Asuha, et al., Nitric acid oxidation of Si to form ultrathin silicon dioxide layers with a low leakage current density,, J. Appl. Phys. 94 (2003) 8.
[11] S. Lindekugel, et al., Plasma hydrogen passivation for crystalline silicon thin-films, in: Proceedings of the 23rd European Photovoltaic Solar Energy Conference, Valencia, Spain, 2008, pp. 2232–2235.
[12] M. Reusch, et al., Fill factor limitation of silicon heterojunction solar cells by junction recombination,, Energy Procedia 38 (2013) 297–304.
[13] R. A. Sinton, A. Cuevas, A quasi-steady-state open-circuit voltage method for solar cell characterization, in: Proceedings of the 16th European Photovoltaic Solar Energy Conference, Glasgow, UK, 2000, pp. 1152–1155.
[14] J. Benick, et al., High efficiency n-type Si solar cells on Al_2O_3-passivated boron emitters,, Appl. Phys. Lett. 92 (2008) 253504/1–3.
[15] K. R. McIntosh, P. P. Altermatt, A freeware 1d emitter model for silicon solar cells, in: 35th IEEE Photovoltaic Specialists Conference, pp. 2188–2193, 2010.
[16] Y.H. Kwark, R.M. Swanson, N-type sipos and poly-silicon emitters,, Solid State Electron. 30 (1987) 1121–1125.
[17] C.M. Maritan, N.G. Tarr, Polysilicon emitter P–N–P transistors,, IEEE Trans. Electron Devices 36 (1989) 1139–1144.
[18] R. Brendel, et al., Recent progress and options for future crystalline silicon solar cells, in: Proceedings of the 28th European Photovoltaic Solar Energy Conference and Exhibition, Paris, France, 2013, pp. 676–690.
[19] T. Yamamoto, et al., Bias temperature instability in scaled p(+) polysilicon gate p-MOSFET's,, IEEE Trans. Electron Devices 46 (1999) 921–926.
[20] S. De Wolf, M. Kondo, Nature of doped a-Si:H/ c-Si interface recombination,, J. Appl. Phys. 105 (2009) 103707.
[21] A. Metz, et al., Industrial high performance crystalline silicon solar cells and modules based on rear surface passivation technology,, Sol. Energy Mater. Sol. Cells 120 (2014) 417–425.
[22] A.G. Aberle, et al., High-efficiency silicon solar cells: fill factor limitations and non-ideal diode behaviour due to voltage-dependent rear surface recombination velocity,, Prog. Photovoltaics Res. Appl. 1 (1993) 133–143.
[23] S. Dauwe, et al., Experimental evidence of parasitic shunting in silicon nitride rear surface passivated solar cells,, Prog. Photovoltaics Res. Appl. 10 (2002) 271–278.
[24] P. Saint-Cast, et al., High-efficiency c-Si solar cells passivated with ALD and PECVD aluminum oxide,, IEEE Electron Device Lett. 31 (2010) 695–697.
[25] J. Schmidt, et al., Surface passivation of high-efficiency silicon solar cells by atomic-layer-deposited Al_2O_3,, Prog. Photovoltaics Res. Appl. 16 (2008) 461–466.
[26] M. Bivour, et al., Doped layer optimization for silicon heterojunctions by injection-level-dependent open-circuit voltage measurements,, IEEE J. Photovoltaics 4 (2014) 566–574.
[27] K. Heilig, Determination of surface properties by means of large-signal photovoltage pulses and influence of trapping,, Surf. Sci. 44 (1974) 421–437.
[28] H.C. Degraaff, J.G. Degroot, Sis tunnel emitter—theory for emitters with thin interface layers,, IEEE Trans. Electron Devices 26 (1979) 1771–1776.
[29] A.A. Eltoukhy, D.J. Roulston, The role of the interfacial layer in polysilicon emitter bipolar-transistors,, IEEE Trans. Electron Devices 29 (1982) 1862–1869.
[30] R. Peibst, et al., A simple model describing the symmetric I-V characteristics of p polycrystalline Si/n monocrystalline Si, and n polycrystalline Si/p monocrystalline Si junctions,, IEEE J. Photovoltaics 4 (2014) 841–850.
[31] W.C. Lee, C.M. Hu, Modeling CMOS tunneling currents through ultrathin gate oxide due to conduction- and valence-band electron and hole tunneling,, IEEE Trans. Electron Devices 48 (2001) 1366–1373.
[32] I.R.C. Post, P. Ashburn, Investigation of boron-diffusion in polysilicon and its application to the design of P–N–P polysilicon emitter bipolar-transistors with shallow emitter junctions,, IEEE Trans. Electron Devices 38 (1991) 2442–2451.
[33] J. Shewchun, et al., Theory of metal-insulator-semiconductor solar cells,, J. Appl. Phys. 48 (1977) 765.
[34] F. Feldmann, et al., Carrier-selective contacts for Si solar cells,, Appl. Phys. Lett. 104 (2014) 4.
[35] D. Pysch, et al., A review and comparison of different methods to determine the series resistance of solar cells,, Sol. Energy Mater. Sol. Cells 91 (2007) 1698–1706.